

## ANALYSIS OF SURFACE EFFECT ON SOLAR-LIKE OSCILLATION FREQUENCIES USING 3D HYDRODYNAMICAL MODELS

T. Sonoi<sup>1</sup>, R. Samadi<sup>1</sup>, K. Belkacem<sup>1</sup>, H.-G. Ludwig<sup>2,3</sup>, E. Caffau<sup>3</sup>  
and B. Mosser<sup>1</sup>

**Abstract.** We evaluate the frequency difference between standard stellar models and models patched with 3D hydrodynamical models across the  $T_{\text{eff}}-g$  plane. It allows us to constrain frequency corrections for surface effect. The coefficients in the correction functionals are thus provided as functions of effective temperature and surface gravity.

### 1 Introduction

The space missions CoRoT and *Kepler* have provided us with a wealth of high-quality data. They helped us improve knowledge of solar-like oscillations significantly. The precise seismic determination of stellar properties is derived from the detection of a large number of consecutive radial orders and angular degrees as well as from the mode identification. However, poor modeling of the near-surface convection leads to incorrect evaluation of oscillation frequencies: this is called surface effect. For the Sun, a systematic discrepancy between observed and model frequencies has been emphasized (*e.g.* Christensen-Dalsgaard *et al.* 1988, 1996). Indeed, precise determination of stellar interiors requires realistic modelling of equilibrium structure and oscillations.

In most cases, the mixing-length theory is used to model convection in computation of stellar evolution. However, we need to account for more complex physical processes, such as turbulence for the near-surface convection. For the Sun, there have been many analyses of the surface effect, most often based on more sophisticated treatment of surface convection. Indeed, the frequencies of the high-order

---

<sup>1</sup> LESIA, Observatoire de Paris, PSL Research University, CNRS, Université Pierre et Marie Curie, Université Denis Diderot, 92195 Meudon, France

<sup>2</sup> Zentrum für Astronomie der Universität Heidelberg, Landessternwarte, Königstuhl 12, D-69117 Heidelberg, Germany

<sup>3</sup> GEPI, Observatoire de Paris, PSL Research University, CNRS, Université Denis Diderot, Sorbonne Paris Cité, 5 Place Jules Janssen, 92195 Meudon, France

$p$  modes were found to be affected by the treatment of convection (*e.g.* Brown 1984). Similar attempts have been carried out using models constructed by 3D hydrodynamical simulations (*e.g.* Rosenthal *et al.* 1999; Piau *et al.* 2014; Ball *et al.* 2016; Magic & Weiss 2016; Houdek *et al.* 2016; Trampedach *et al.* 2016). It has been found that turbulent pressure, neglected in standard models, plays an important role since it elevates the outer layers and, as a result, oscillation frequencies are decreased.

In the absence of any definitive treatments for the surface effect in standard models, Kjeldsen *et al.* (2008) proposed an empirical power law to correct model frequencies. They provided the value of the power index in the power law,  $b = 4.9$ , by analyzing the difference between the observed solar frequencies and the ones of Model S (Christensen-Dalsgaard *et al.* 1996). Since then, this value has been adopted to correct frequencies of stars other than the Sun (*e.g.* Christensen-Dalsgaard *et al.* 2010). Indeed, the frequency correction is required since, without it, it is difficult to find a good model from comparison with observations. At this stage, however, we still lack a physical justification for this treatment.

Thus, we aim to physically constrain the frequency correction using a grid of outer-layer models constructed by 3D hydrodynamical simulations across the HR diagram.

## 2 Patched models and eigenfrequencies

We used 3D hydrodynamical models of outer layers of solar-like stars obtained by the CO<sup>5</sup>BOLD code (Freytag *et al.* 2012) with the CIFIST grid (Ludwig *et al.* 2009). The adopted chemical mixture is similar to the solar abundances determined by Asplund *et al.* (2005). We used 10 models having different effective temperature,  $T_{\text{eff}}$ , and gravity acceleration at the photosphere,  $g$ , as shown in Figure 2. We performed temporal and horizontal averages at constant geometrical depth for the 3D models.

Following Trampedach (1997) and Samadi *et al.* (2007, 2008), we constructed an unpatched model (UPM) and a patched model (PM) corresponding to each 3D model. The UPM was obtained using the CESTAM stellar evolution code (Marques *et al.* 2013) by matching  $T_{\text{eff}}$ ,  $g$  and the temperature at the level where the total pressure is equal to that at the bottom of the averaged 3D model. The matching was performed through a Levenberg-Marquardt algorithm with three free parameters: the stellar age, the total mass,  $M$ , and the mixing length parameter,  $\alpha_{\text{MLT}}$ . For models in the post-main sequence stage (H, I and J in Fig. 2), the central temperature rather than the age was considered as a free parameter because of their rapid evolution. Convection in the 1D models is treated using the standard mixing-length theory (Böhm-Vitense 1958) and does not include turbulent pressure. The Eddington gray  $T - \tau$  law was used for the atmosphere of UPMs.

Subsequently, the UPMs and averaged 3D models were matched to construct the PMs. The additional support of turbulent pressure modifies the hydrostatic equilibrium, so that the radius of PM is larger by 0.01 to 0.2% than UPM. The

difference in radius between PM and UPM increases with increasing  $T_{\text{eff}}$  or with decreasing  $g$  due to the increasing contribution of turbulent pressure.

We computed frequencies of the PMs and UPMs using the ADIPLS code (Christensen-Dalsgaard 2008). We consider only radial modes below the acoustic cut-off frequency. For the PMs, we adopt the gas-gamma model (GGM) approximation, which is one of adiabatic approaches for models including turbulent pressure proposed by Rosenthal *et al.* (1999). In this approximation, the relative Lagrangian perturbation of turbulent pressure,  $\delta p_{\text{turb}}/p_{\text{turb}}$ , is assumed to equal that of gas pressure,  $\delta p_g/p_g$ . Indeed, this approximation is a physically crude way to take  $\delta p_{\text{turb}}$  into account, and another approximation proposed by Rosenthal *et al.* (1999) the reduced-gamma (RGM) approximation, which imposes  $\delta p_{\text{turb}} = 0$ , has been preferred to use by some authors (*e.g.* Houdek *et al.* 2016; Trampedach *et al.* 2016). Nevertheless, Rosenthal *et al.* found that the GGM gives a better agreement with the observed frequencies, and it has been also adopted by previous studies (*e.g.* Piau *et al.* 2014; Ball *et al.* 2016; Magic & Weiss 2016). An appropriate way to include  $\delta p_{\text{turb}}$  in the computation of adiabatic oscillations is investigated by Sonoi *et al.* (2016) using a time-dependent convection formalism.

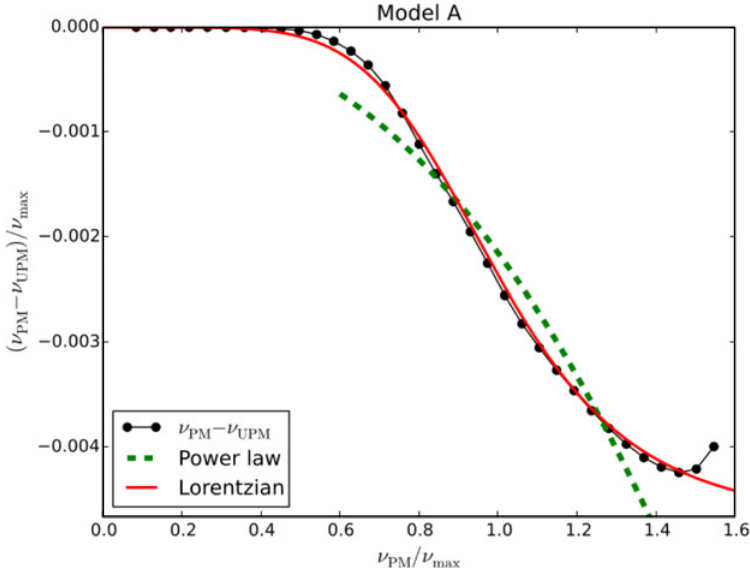
### 3 Functional fittings to frequency difference between PM and UPM

Figure 1 shows the difference in radial-mode frequencies between the PM and UPM for Model A, which is close to the Sun ( $T_{\text{eff}} = 5775$  K,  $\log g = 4.44$ ). The frequencies are divided by  $\nu_{\text{max}}$ , which is estimated by the scaling relation  $\nu_{\text{max}} \propto gT_{\text{eff}}^{-1/2}$  while adopting  $\nu_{\text{max},\odot} = 3100 \mu\text{Hz}$ ,  $\log g_{\odot} = 4.438$ , and  $T_{\text{eff},\odot} = 5777$  K for solar values. As discussed in Section 2, PM has a larger radius than UPM due to the elevation of the outer layers by turbulent pressure. The cavity where acoustic waves propagate then becomes larger, and the mode frequencies become lower for PM. As a consequence, the value  $(\nu_{\text{PM}} - \nu_{\text{UPM}})/\nu_{\text{max}}$  is negative for all the models. We can also see that the difference becomes greater with increasing frequency. As the frequency becomes higher, the mode propagates farther in the outer region, so that it is affected by the surface effect more strongly.

To constrain the frequency corrections of standard stellar models, we fitted the correction functionals to frequency differences between PM and UPM. Since the PMs include realistic profiles of the upper layers, we consider their oscillation frequencies to be the observed ones. Therefore, the frequency differences can be regarded as the predicted frequency errors of standard stellar models. We fitted a power-law function based on Kjeldsen *et al.* (2008),

$$\frac{\delta\nu}{\nu_{\text{max}}} = a \left( \frac{\nu_{\text{PM}}}{\nu_{\text{max}}} \right)^b, \quad (3.1)$$

to the frequency differences.  $\delta\nu$  is the correction of the frequencies, corresponding to  $\nu_{\text{PM}} - \nu_{\text{UPM}}$ .  $a$  and  $b$  are free parameters, and determined by a least-square fitting to the frequency difference. Figure 1 shows a fit to the frequency differences in case of Model A within the range  $0.6 < \nu/\nu_{\text{max}} < 1.4$  (the green dashed line).



**Fig. 1.** Frequency differences of radial modes between PM and UPM divided by  $\nu_{\max}$  as a function of  $\nu_{\text{PM}}/\nu_{\max}$  (black solid line with dots) for Model A ( $T_{\text{eff}} = 5775 \text{ K}$ ,  $\log g = 4.44$ ). The green dashed line and red solid line are least-square fittings with the Kjeldsen *et al.* (2008) power law (Eq. (3.1)) in the range  $0.6 < \nu/\nu_{\max} < 1.4$  and with the modified Lorentzian (Eq. (3.2)) in the whole frequency range, respectively.

The power-law function is not useful for fitting in the whole range. This is the case also for models other than Model A (see Sonoi *et al.* 2015 for details). We chose the above range taking into account the fact that the solar-like oscillations are detected symmetrically about  $\nu_{\max}$ . Nevertheless, the deviation from the frequency difference profile is still substantial.

Then, we propose another formulation based on a Lorentzian function,

$$\frac{\delta\nu}{\nu_{\max}} = \alpha \left[ 1 - \frac{1}{1 + (\nu_{\text{PM}}/\nu_{\max})^\beta} \right]. \quad (3.2)$$

Similarly to  $a$  and  $b$ ,  $\alpha$  and  $\beta$  are free parameters which should be determined by a least-square fitting to the frequency differences between PM and UPM. As shown in Figure 1, this Lorentzian formulation fits well to the frequency differences in the whole frequency range.

Figure 2 shows the values of  $\alpha$  and  $\beta$  obtained by the least-square fittings to the frequency differences between PMs and UPMS corresponding to all the 3D models. The trends of  $a$  and  $b$  with  $T_{\text{eff}}$  and  $g$  are similar to those of  $\alpha$  and  $\beta$  respectively. Indeed, Equation (3.2) reduces to Equation (3.1) in the low-frequency

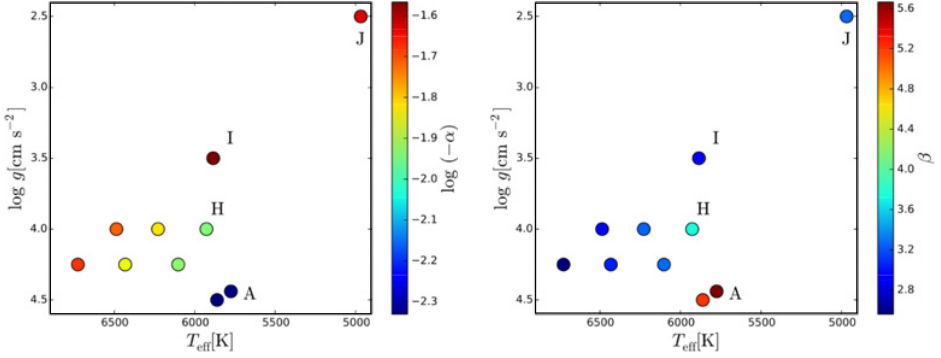


**Fig. 2.** Values of  $\log(-\alpha)$  and  $\beta$  evaluated by the least-square fittings with Equation (3.2) to the frequency differences between PMs and UPMs corresponding to the 10 3D models.

limit,  $\nu/\nu_{\max} \ll 1$ . A least-square fit in the  $T_{\text{eff}} - g$  plane provides the following formulations:

$$\log(-a) = 8.13 \log T_{\text{eff}} - 0.653 \log g - 30.3 \quad (3.3)$$

$$\log b = -3.84 \log T_{\text{eff}} + 0.221 \log g + 13.8, \quad (3.4)$$

for the power-law function (Eq. (3.1)) fit in the range  $0.6 < \nu/\nu_{\max} < 1.4$  and

$$\log(-\alpha) = 7.69 \log T_{\text{eff}} - 0.629 \log g - 28.5, \quad (3.5)$$

$$\log \beta = -3.86 \log T_{\text{eff}} + 0.235 \log g + 14.2, \quad (3.6)$$

for the Lorentzian function (Eq. (3.2)) fit in the whole frequency range.

The absolute values of  $a$  and  $\alpha$  increase with increasing  $T_{\text{eff}}$  or with decreasing  $g$ .  $a$  and  $\alpha/2$  are the values of  $\delta\nu/\nu_{\max}$  at  $\nu = \nu_{\max}$  by definition. Thus, they define the representative scale for  $\delta\nu/\nu_{\max}$ . As mentioned in Section 2, the difference in radius between PM and UPM increases with increasing  $T_{\text{eff}}$  or with decreasing  $g$  due to the contribution of turbulent pressure. It increases the frequency difference and hence the absolute value of  $a$  and  $\alpha$ .

Conversely,  $b$  and  $\beta$  decrease with increasing  $T_{\text{eff}}$  or with decreasing  $g$ . This trend also can be explained in terms of turbulent pressure (see Sonoi *et al.* 2015 for details). Particularly, we see that  $b$  varies substantially with  $T_{\text{eff}}$  and  $g$  although the solar-calibrated value,  $b = 4.9$ , has been adopted to different solar-like stars in previous studies.

## 4 Conclusion

Using a grid of 3D hydrodynamical models, we found that the power index of the Kjeldsen *et al.* (2008) power law (Eq. (3.1)) varies with effective temperature and surface gravity although it has been fixed to the solar-calibrated value in

many previous studies. Besides, we found that the modified Lorentzian formulation (Eq. (3.2)) is more suitable for the frequency errors of standard models predicted with the 3D models. In the following work, we will pursue this problem by considering the effects of nonadiabaticity and time-dependent processes between convection and oscillation, which are expected to be also important for the solar-like oscillation frequencies.

## References

- Asplund, M., Grevesse, N., & Sauval, A.J., 2005, ASP Conf. Ser., 336, 25
- Ball, W.H., Beeck, B., Cameron, R.H., *et al.*, 2016, *ArXiv e-prints*, astro-ph:1606.02713
- Böhm-Vitense, E., 1958, Z. Astrophysik, 46, 108
- Brown, T.M., 1984, Science, 226, 687
- Christensen-Dalsgaard, J., Dappen, W., & Lebreton, Y., 1988, Nature, 336, 634
- Christensen-Dalsgaard, J., Dappen, W., Ajukov, S.V., *et al.*, 1996, Science, 272, 1286
- Christensen-Dalsgaard, J., 2008, Ap&SS, 316, 113
- Christensen-Dalsgaard, J., Kjeldsen, H., Brown, T.M., *et al.*, 2010, ApJ, 713, L164
- Freytag, B., Steffen, M., Ludwig, H.-G., *et al.*, 2012, J. Comput. Phys., 231, 919
- Houdek, G., Trampedach, R., Aarslev, M.J., *et al.*, 2016, *ArXiv e-prints*, astro-ph:1609.06129
- Kjeldsen, H., Bedding, T.R., & Christensen-Dalsgaard, J., 2008, ApJ, 683, L175
- Ludwig, H.-G., Caffau, E., Steffen, M., *et al.*, 2009, Mem. Soc. Astron. Ital., 80, 711
- Magic, Z., & Weiss, A., 2016, A&A, 592, A24
- Marques, J.P., Goupil, M.J., Lebreton, Y., *et al.*, 2013, A&A, 549, 74
- Piau, L., Collet, R., Stein, R.F., *et al.*, 2014, MNRAS, 437, 164
- Rosenthal, C.S., Christensen-Dalsgaard, J., Nordlund, A.A., *et al.*, 1999, A&A, 351, 689
- Samadi, R., Georgobiani, D., Trampedach, R., *et al.*, 2007, A&A, 463, 297
- Samadi, R., Belkacem, K., Goupil, M.J., *et al.*, 2008, A&A, 489, 291
- Sonoi, T., Samadi, R., Belkacem, K., *et al.*, 2015, A&A, 583, A112
- Sonoi, T., Belkacem, K., Dupret, M.-A., *et al.*, 2016, A&A, submitted
- Trampedach, R., 1997, *Master Thesis*, Aarhus University
- Trampedach, R., Aarslev, M.J., Houdek, G., *et al.*, 2016, *ArXiv e-prints*, astro-ph:1611.02638